

Mechanism of the Chemical Deposition of Nickel on Silicon Wafers in Aqueous Solution

Nao Takano, Naohiro Hosoda, Taro Yamada,* and Tetsuya Osaka**^z

Department of Applied Chemistry, School of Science and Engineering, Kagami Memorial Laboratory for Materials Science and Technology, Waseda University, Tokyo 169-8555, Japan

The deposition of metallic nickel on n-Si(100) wafers was performed without external potential control in aqueous NiSO₄ solutions of different compositions at pH 8.0. Without giving any catalyzation treatment, the deposition of nickel on hydrogen-terminated Si(100) was confirmed in a conventional electroless plating bath containing NaH₂PO₂ as the reducing agent, sodium citrate as the complexing agent, and (NH₄)₂SO₄ as the buffering agent. The deposition of nickel was found to take place also in a bath without the reducing agent, and even in a simple solution consisting of NiSO₄ and (NH₄)₂SO₄. By using a transmission electron microscope equipped with an energy dispersive X-ray spectrometer, the cross sections of the films deposited from these solutions were examined, which revealed formation of silicon oxide between the Ni deposit and Si substrate. Based on these results, the mechanism of the entire process of electroless Ni deposition on Si is discussed.

© 1999 The Electrochemical Society. S0013-4651(98)06-101-1. All rights reserved.

Manuscript submitted June 29, 1998; revised manuscript received November 15, 1998.

Various techniques are available for forming metal films on substrates, such as chemical vapor deposition (CVD), sputtering, evaporation, electrodeposition, and electroless deposition. Among these techniques, electroless deposition has been attracting attention because of its simplicity in operation and its low cost. In the semiconductor-device industry, attempts have been made to utilize the method of electroless deposition for delineating semiconductor junctions,^{1,2} making ohmic contacts,³ and micropatterning integrated circuits.⁴

In the past several years, filling via holes and trenches^{5,6} have been attempted for producing ultralarge scale integration (ULSI) interconnects.^{7,8} In this case, electroless deposition is more attractive than dry processes such as CVD and sputtering because of the simplicity and the via hole filling ability of the former method.

Furthermore, metal dots of approximately 10 nm diam can be fabricated on Si wafers by electroless deposition, which has a great potential for realization of ultrahigh density (over 1 terabit cm⁻²) read-only memory (ROM) or random-access memory (RAM)⁹ devices. Ion implantation by using a focused ion beam apparatus was found to modify the silicon surface and initiate electroless gold deposition.¹⁰ We believe that such a phenomenon can be utilized to make small metal dots on silicon surfaces.

A project entitled "Wafer-Scale Formation Process of Quantum Dots" was started under the sponsorship of the Research for the Future project, The Japan Society for the Promotion of Science. As part of the initial phase of this project, we have investigated the possibility of depositing small metal dots on silicon by wet processes. Results of our preliminary investigation were reported elsewhere.¹¹

Electroless metal deposition on Si wafer was investigated by several researchers.^{2,5,12-15} In most of those studies, an HF-containing electrolyte was used.^{2,12-15} In this study, an alkaline aqueous solution without F⁻ was used instead, and the nickel deposition mechanism on silicon was examined. For the purpose of the mechanistic study described in this paper, the composition of the electroless deposition bath was simplified to clarify the mode of participation of Si in the metal deposition. The electron microscopic analyses were performed to observe the surfaces and cross sections of specimens.

Experimental

The substrates used were n-type Si(100) wafers (phosphorus-doped with a resistivity of 8 to 12 Ω cm, Shin-Etsu Handotai Co., Ltd.). The specimens were 2 × 2 cm square pieces cut out of the wafer. They were cleaned by the RCA method,¹⁶ which is one of the standard cleaning procedures for Si wafers. After cleaning, these wafers were rinsed in distilled water with the resistivity of 1.5 × 10⁶ ~ 2.0 × 10⁶ Ω cm, which was used in all stages of experiment. When necessary, catalyzation of Si wafer was performed by simple

immersion in an aqueous PdCl₂ solution (0.1 g dm⁻³ of PdCl₂ in dilute HCl) for 10 s immediately before immersion in the electroless deposition bath.

For the chemical deposition of nickel, three types of baths listed in Table I were employed. Bath A was a typical NiP electroless deposition bath,^{17,18} operated at 80°C and pH 8.0 adjusted with NH₄OH. The reducing agent, NaH₂PO₂, was excluded in baths B and C. Bath B contained Ni²⁺ with sodium citrate as the complexing agent for Ni²⁺, and (NH₄)₂SO₄ as the buffering agent. Bath C contained Ni²⁺ with only (NH₄)₂SO₄ and no complexing agent. Baths B and C were both operated at the same condition as bath A. All deposition experiments were performed on a class 100 clean bench.

The deposited specimens were examined by using both a field emission transmission electron microscope (FETEM; Hitachi, Ltd., HF-2000) equipped with an energy dispersive X-ray spectrometer (EDX; Kevex Instruments, Inc., Sigma), and a scanning electron microscope (SEM; Hitachi, Ltd., S-2500CX). The samples for the cross-sectional FETEM observation were prepared by a submicrometer-scale fabrication technique using a focused ion beam machine (FIB; Hitachi, Ltd., FB-2000A). An electron probe microanalyzer (EPMA; JEOL Ltd., JXA-8600) was used for elemental analysis of the deposits.

Results and Discussion

Ni deposition on an uncatalyzed silicon wafer.—The nature of nickel deposition on Si wafer was first examined. First, NiP electroless plating was performed on a Si wafer with the catalyzation.^{17,18} When bath A was used, phosphorus was included in the deposit because this bath contained NaH₂PO₂ as the reducing agent. Therefore, we use the terms NiP and Ni to differentiate the deposits produced in bath A from those produced from baths B and C, respectively.

Although the NiP film was clearly formed in bath A, the film peeled off easily upon rinsing in water. On the other hand, when plating was done in bath A without catalyzation, a more adherent

Table I. Bath compositions and operating conditions.

Chemicals (mol dm ⁻³)	Bath A	Bath B	Bath C
NiSO ₄ ·6H ₂ O	0.10	0.10	0.10
NaH ₂ PO ₂ ·H ₂ O	0.15	—	—
(NH ₄) ₂ SO ₄	0.50	0.50	0.50
Sodium citrate	0.20	0.20	—

pH was 8.0 (adjusted with NH₄OH).
Temperature was 80°C for all baths.

* Electrochemical Society Active Member.

^z E-mail: osakatet@mn.waseda.ac.jp

metallic film was deposited on the wafer, and this film was confirmed to consist mainly of nickel and phosphorus by EPMA. In the latter case, the metallic film did not peel off upon rinsing. From the SEM images in Fig. 1, the formation of an NiP deposit from bath A was confirmed on the uncatalyzed wafer. This result suggests that the nickel deposition in this case did not proceed by the conventional electroless plating mechanism, i.e., silicon itself is not a catalyst for the electroless nickel deposition reaction, and, nevertheless, the deposition reaction started without catalyzing the silicon.

From these results, we believe that the mechanism of the initial deposition of nickel on Si wafer is different for the two different cases, namely, with and without the presence of the palladium catalyst.

To understand the initial deposition reaction of electroless NiP plating on uncatalyzed Si wafer, we prepared baths B and C without the reducing agent of NaH_2PO_2 . In bath C, sodium citrate was also excluded (see Table I).

Figure 2 shows SEM micrographs of Si(100) after treatment in bath B. The deposition rate in bath B was much slower than that in bath A, as clearly seen by comparing the ranges of immersion time used to obtain deposits shown in Fig. 1 and 2 (see respective figure captions). Nevertheless, nickel deposition did clearly take place from bath B, as was confirmed by EPMA. In the case of bath B, the deposited grains did not grow in size as significantly as did those from bath A.

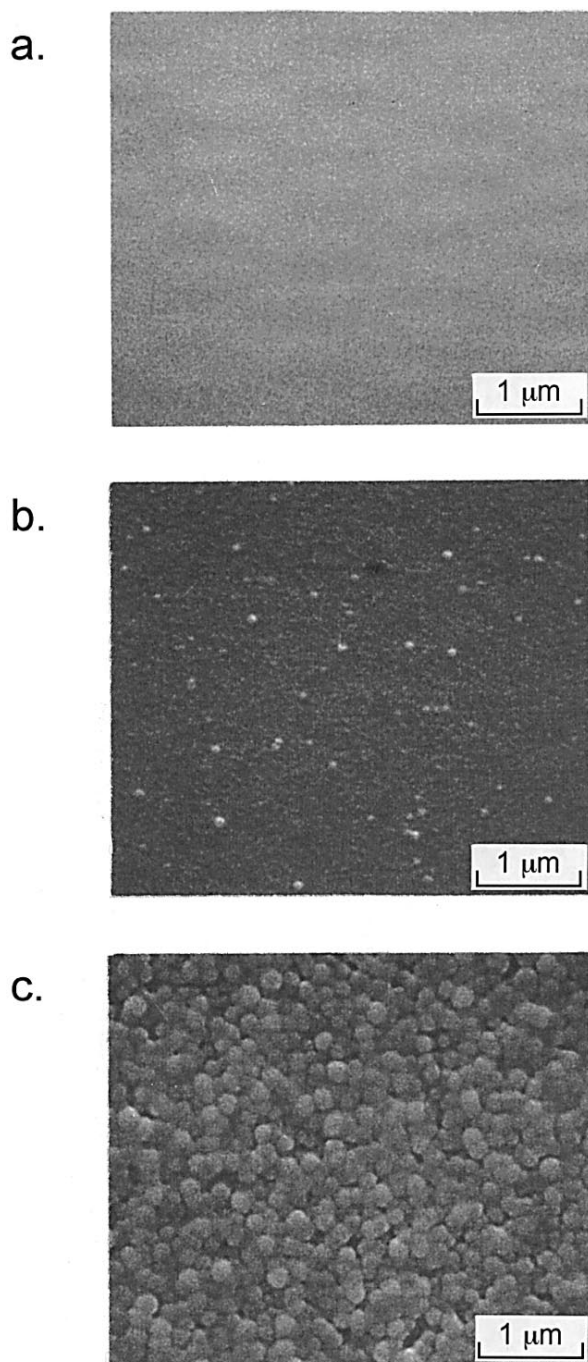


Figure 1. SEM micrographs of NiP deposits produced on RCA-pretreated Si(100) from bath A (electroless NiP bath) at pH 8.0 and 80°C at various deposition times: (a) 10, (b) 30, and (c) 60 s.

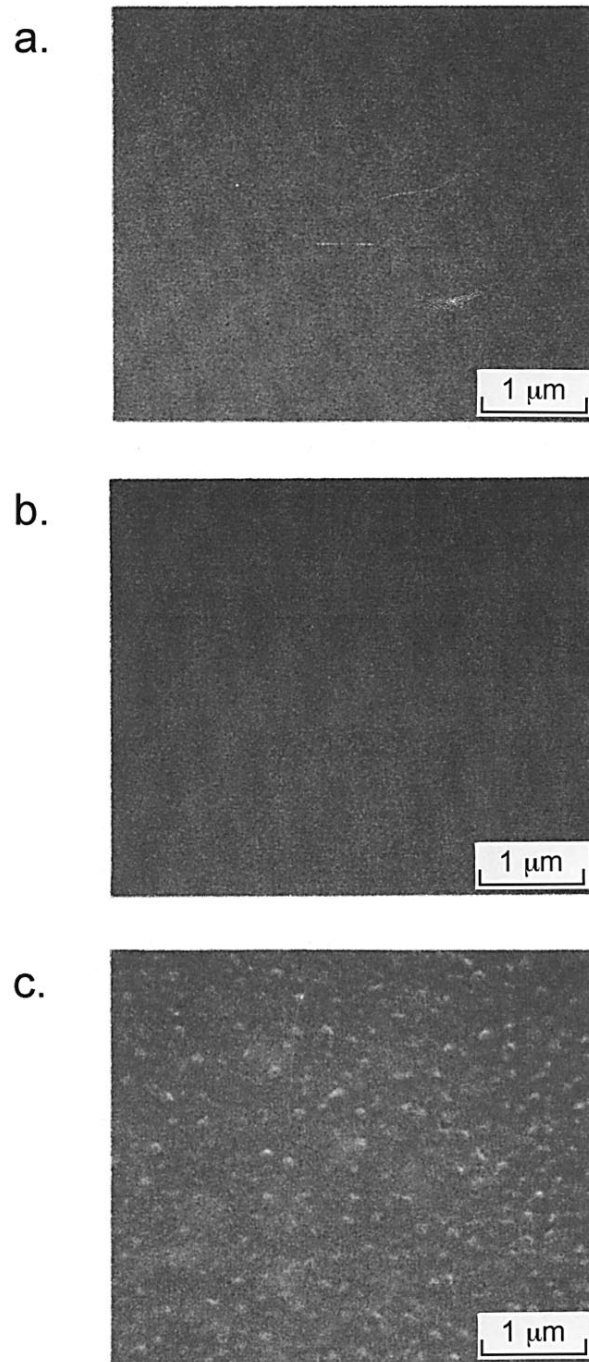


Figure 2. SEM micrographs of Ni deposits produced on RCA-pretreated Si(100) from bath B (without reducing agent) at pH 8.0 and 80°C at various deposition times: (a) 5, (b) 10, and (c) 30 min.

The quantity of Ni deposit obtained from bath C was clearly greater than that from bath B. Figure 3 shows SEM micrographs of the Si(100) surface treated in bath C. This result implies that the reduction of nickel ion is restrained by citrate anions, which have a strong ability to coordinate with Ni^{2+} .

To clarify this effect of citrate, electrochemical measurements were performed in the potentiostatic mode with a Ag/AgCl reference electrode and a Pt wire counter electrode. Figure 4 shows current-potential curves obtained with a Si(100) electrode in baths B and C. The dotted line represents background current in the electrolyte containing no Ni^{2+} . The cathodic currents in baths B and C are, hence,

due to the electrochemical reduction of Ni^{2+} . It is seen that the Ni deposition from bath B, which contained sodium citrate, occurred at more negative potentials than that from bath C, indicating that the electrodeposition of Ni is retarded by the complexation with citrate in bath B. This result corresponds well to the chemical deposition rates indicated in Fig. 2 and 3.

In view of the results obtained with baths B and C, it is apparent that the reaction of the initial Ni deposition from bath A does not involve the reducing agent, NaH_2PO_2 , i.e., it should be similar to the reaction in baths B and C. After the initial stage, the NiP deposition in bath A must proceed by the autocatalytic reaction on deposited metallic Ni involving the reducing agent.

The mechanism of chemical nickel deposition on silicon wafer.— The electrodeposition of Ni from Ni^{2+} takes place with the transfer of electrons supplied by an external source of current. On the other hand, for the chemical deposition of Ni on Si, an alternate mechanism to supply electrons must be considered. We hypothesized three different mechanisms described below.

The first conceivable mechanism is that the nickel deposition takes place through the displacement of surface hydrogen atoms that terminate the Si surface. This mechanism is schematized in Fig. 5a. Calculations using Nernst equations show that the redox potential for the Ni^{2+} ($a_{\text{Ni}^{2+}} = 0.1$)-Ni couple is -0.27 V vs. normal hydrogen electrode (NHE) at 80°C , and that of the hydrogen elimination reaction ($\equiv\text{Si}-\text{H} \rightarrow \equiv\text{Si}^* + \text{H}^+ + \text{e}^-$) is -0.73 V vs. NHE at pH 8.0 and 80°C .¹⁹ Although the mechanism of the chemical deposition by galvanic displacement is complex and involves various other factors, the above calculated potential values indicate that nickel deposition by the galvanic displacement between Ni^{2+} and $\equiv\text{Si}-\text{H}$ is thermodynamically feasible. In this mechanism, it is anticipated that the Ni atoms produced initially should form a monolayer. Our experimental results, however, show that the Ni layers formed in bath B or C were not single monolayers as is clearly seen in Fig. 2 and 3. Thus, this mechanism can hardly be responsible for the major initial deposition reaction. It is still possible that the Ni deposition at the very initial stages occur by displacement of terminating H atoms by Ni^{2+} .

The second mechanism we considered is based on the photochemical reaction as represented by the schematic drawing in Fig. 5b. In this mechanism, Ni is deposited cathodically by the electrons which are made available through the photoexcitation in sili-

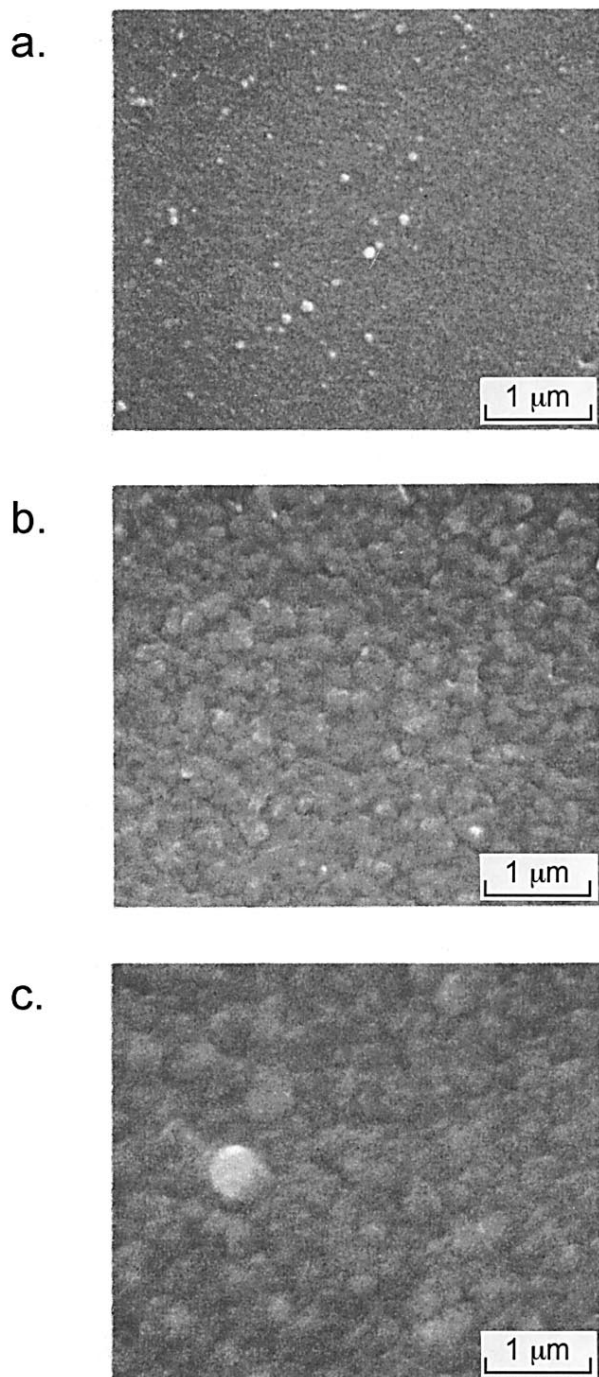


Figure 3. SEM micrographs of Ni deposits produced on RCA-pretreated Si(100) from bath C (without reducing agent and complexing agent) at pH 8.0 and 80°C at various deposition times: (a) 5, (b) 10, and (c) 30 min.

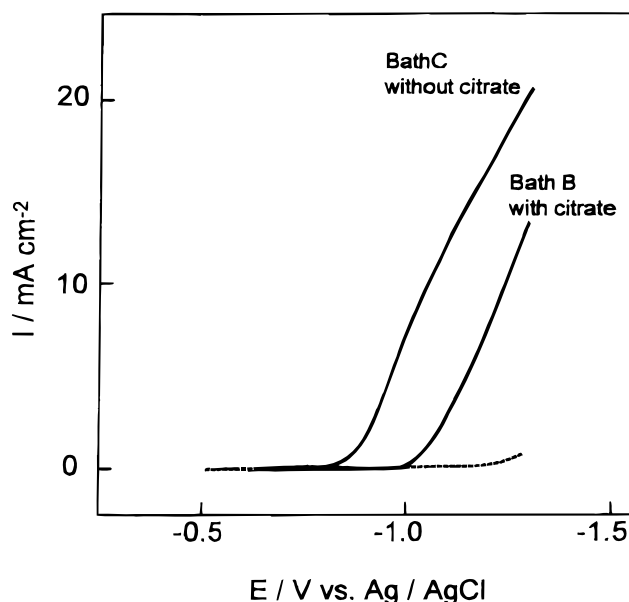


Figure 4. Current-potential curves of Si(100) in baths B and C, and background curve, all recorded at pH 8.0 and 80°C with 2 mV s^{-1} . The Ag/AgCl reference electrode was also maintained at 80°C .

con. Simultaneously, O_2 is generated by the anodic reaction since electrons are injected from hydroxide ions into the valence band of silicon. To investigate the applicability of this mechanism, experiments were performed in the dark and under illumination of room light. If this mechanism were operative, Ni deposition would hardly occur in the dark. However, no difference was noted between the two cases of with and without illumination. This result shows that the second mechanism is not valid.

The third mechanism we considered is that the reduction of Ni^{2+} proceeds through the galvanic displacement of silicon in the alkaline aqueous solution. In other words, nickel ion receives electrons released by the electrochemical oxidation of Si^{20} as schematically illustrated in Fig. 5c. To verify this mechanism, it was thought necessary to identify the final product of Si after ejection of the electrons. It was considered that significant information should be obtainable by examining the cross section of the interface between the silicon substrate and the nickel deposit in the initial stages of the reaction.

To observe the reaction products in detail, the cross section of a sample obtained from bath C was investigated by FETEM (the accelerating voltage used was 200 kV). The minimum electron-beam diameter of FETEM was 5 nm. The sample for cross-sectional FETEM observation was prepared by using FIB, and it was fabricated with a thickness of less than 0.1 μm . The images are shown in Fig. 6a. Note that the black area in the upper part of the image shows the tungsten which was deposited by CVD to protect the sample surface from ion etching. The white area under the tungsten is the carbon layer evaporated to make the surface conductive for scanning ion beam irradiation. The gray area at the bottom portion of the image is the Si substrate, and the black area between carbon and Si is the Ni deposit.

An elemental analysis of this interfacial region was carried out by FETEM equipped with EDX. The minimum electron-beam spot

diameter in the EDX analysis was 0.5 nm. Figure 6b displays a higher magnification FETEM image of the part pointed out by the arrow in Fig. 6a. Elemental analysis was carried out at five different locations marked 1 through 5 in Fig. 6b. The results of EDX analysis are summarized in Fig. 7. It is clearly seen that a significant amount of oxygen was present between the Si substrate and the Ni deposit. These results indicate that the white area located between Si and Ni in Fig. 6a mainly consisted of silicon oxide with a thickness of ca. 20 nm. Such a silicon oxide layer was not found on the bare n-Si(100) surface prepared by the RCA process, which includes treatment with an aqueous solution of HF. For a specimen immediately after the HF treatment, it was confirmed by Auger electron spectroscopy that there was no silicon oxide layer present on the surface.

From these results, we emphasize that the formation of the silicon oxide layer is a direct result of the chemical deposition of nickel in the absence of the reducing agent. In Fig. 8, the detailed mechanism of nickel deposition is illustrated. After the nucleation of nickel (steps 2 and 3), the electrons released by the oxidation of silicon are supplied to nickel ions through the deposited nickel metal (step 4), resulting in the growth of crystals of nickel metal. The oxide layer which was observed between the Ni deposit and the substrate (Fig. 6a) seems to be produced as a result of the reaction of oxidized Si with OH^- ions, which is promoted by Ni^{2+} ions. These results show that the reactivity of Si toward the galvanic displacement reaction plays an important role in the chemical deposition of Ni. It is of interest to note that, very recently, Kim et al. found that the deposi-

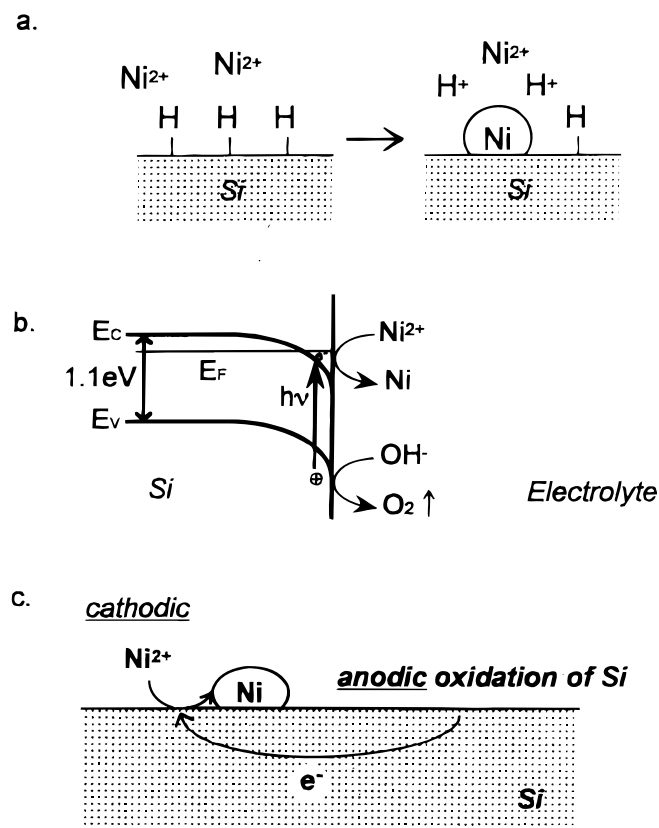


Figure 5. Three plausible mechanisms considered for the Ni deposition on silicon surfaces without reducing agent: (a) displacement of surface H-terminated Si surface, (b) the photochemical reaction, and (c) anodic oxidation of silicon and cathodic reduction of nickel ion.

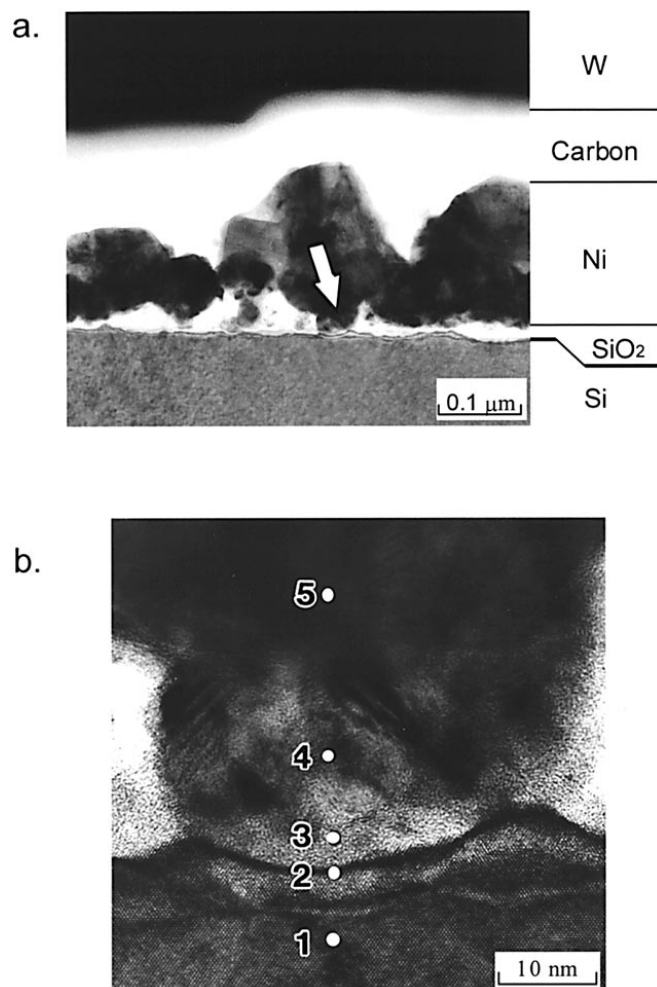


Figure 6. (a) Cross-sectional FETEM image of Si(100) obtained from bath C, (b) higher magnification FETEM image. The numbers represent locations where elemental analysis was carried out. The minimum electron-beam diameter used in the FETEM observation was 5 nm.

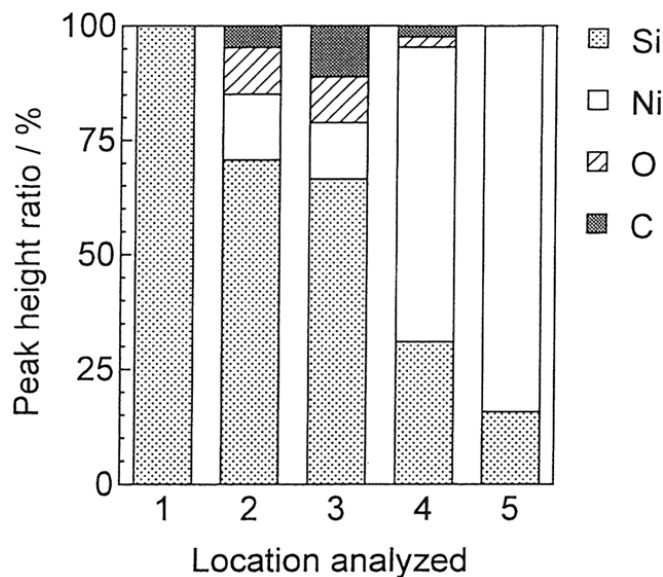


Figure 7. Peak height ratios of EDX spectra of Fig. 6. The numbers on abscissa correspond to those in Fig. 6b. The minimum electron-beam spot diameter in the EDX analysis was 0.5 nm.

tion of Cu on Si from solutions containing Cu^{2+} ions as an impurity is accompanied by the formation of an SiO_2 layer.^{21,22}

On the basis of all of the results described above, we conclude that the nickel deposition from bath A on uncatalyzed silicon proceeds in two consecutive steps. In the first step, the reduction of Ni^{2+} is initiated by the mechanism of galvanic displacement with silicon substrate. In the second step, the nickel deposition proceeds autocatalytically by the reaction with the reducing agent. We confirmed that nickel deposition does take place on n-Si(100) surface from the simple bath C.

This work is expected to contribute to the development of key processes for the metallic quantum nanocluster formation required in the future technology of fabrication of ultrahigh density ROM.

Conclusion

The NiP deposition on RCA-pretreated and uncatalyzed n-Si(100) surfaces was confirmed to take place from a conventional electroless NiP bath as well as from baths containing NiSO_4 but no reducing agent. It is apparent that the Ni deposition in the bath consisting only of NiSO_4 and $(\text{NH}_4)_2\text{SO}_4$ proceeds by a mechanism different from that of the usual electroless deposition. The Ni deposition is accompanied by the formation of silicon oxide. The results of this study can be utilized for the formation of small metal dots on silicon surfaces, which are needed for the fabrication of ultrahigh density ROM devices.

Acknowledgment

This work was financially supported by the Research for the Future project "Wafer-Scale Formation Process of Quantum Dots" of the Japan Society for the Promotion of Science, and by a Grant-in-Aid for Scientific Research on Priority Area of Electrochemistry of Ordered Interfaces from the ministry of Education, Science, Sports and Culture, Japan. The authors thank the experimental support of Application Technology Dept., Techno Research Laboratory, Hitachi Instruments Engineering Co., Ltd. for FIB sample preparation and FETEM analysis.

T. Osaka assisted in meeting the publication costs of this article.

References

- H. Iwasa, M. Yokozawa, and I. Teramoto, *J. Electrochem. Soc.*, **115**, 485 (1968).
- H. Cachet, M. Froment, and E. Souteyrand, *J. Electrochem. Soc.*, **139**, 2920 (1992).
- M. V. Sullivan and J. H. Eiger, *J. Electrochem. Soc.*, **104**, 226 (1957).
- J. M. Calvert, G. S. Calabrese, J. F. Bohland, M. Chen, W. J. Dressick, C. S. Dulcey, J. H. George, Jr., J. Kosakowski, E. K. Pavelcheck, K. W. Rhee, and L. M.

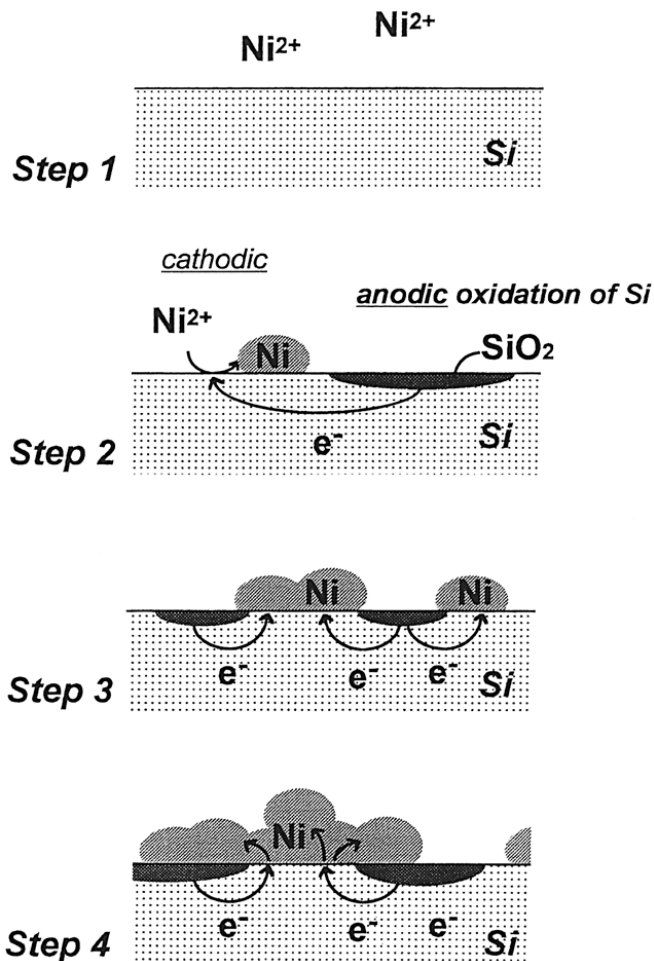


Figure 8. Schematic representation of the mechanism for the Ni deposition on Si from the bath without the reducing agent.

- Shirey, *J. Vac. Sci. Technol., B*, **12**, 3884 (1994).
- C. H. Ting, Abstract 512, p. 720, The Electrochemical Society Extended Abstracts, Vol. 87-2, Honolulu, HI, Oct 18-23 (1987); C. H. Ting, *Electroless Deposition of Metals and Alloys*, M. Paunovic and I. Izumi, Editors, PV 88-12, p. 223, The Electrochemical Society Proceedings Series, Pennington, NJ (1988); C. H. Ting and M. Paunovic, *J. Electrochem. Soc.*, **136**, 456 (1989).
- C. H. Ting, M. Paunovic, P. L. Pai, and G. Chin, *J. Electrochem. Soc.*, **136**, 462 (1989).
- M. J. Desilva and Y. Shacham-Diamand, *J. Electrochem. Soc.*, **143**, 3512 (1996).
- V. M. Dubin, Y. Shacham-Diamand, B. Zhao, P. K. Vasudev, and C. H. Ting, *J. Electrochem. Soc.*, **144**, 898 (1997).
- C. Y. Chou, *J. Magn. Soc. Jpn.*, **21**, 1023 (1997).
- T. Shiiba, K. Hara, M. Fukasawa, H. Sakuma, M. Takai, T. Osaka, and I. Ohdomari, in *Proceedings of the 43rd Spring Meeting of the Japan Society of Applied Physics and Related Societies*, p. 531, Japan Society of Applied Physics, Tokyo (1996).
- T. Osaka, N. Takano, and S. Komaba, *Chem. Lett.*, **7**, 657 (1998).
- L. A. Nagahara, T. Ohmori, K. Hashimoto, and A. Fujishima, *J. Electroanal. Chem.*, **333**, 363 (1992).
- L. A. Nagahara, T. Ohmori, K. Hashimoto, and A. Fujishima, *J. Vac. Sci. Technol., A*, **11**, 763 (1993).
- P. Gorostiza, J. Servat, and F. Sanz, *Thin Solid Films*, **275**, 12 (1996).
- P. Gorostiza, R. Diaz, J. Servat, F. Sanz, and J. R. Morante, *J. Electrochem. Soc.*, **144**, 909 (1997).
- W. Kern and D. A. Puotinen, *RCA Rev.*, **31**, 187 (1970).
- T. Osaka and I. Koiwa, *Kinzoku Hyoumen Gijyutu (J. Surf. Finish. Soc. Jpn.)*, **34**, 330 (1983).
- Y. Okinaka and T. Osaka, in *Advances in Electrochemical Science and Engineering*, H. Gerischer and C. W. Tobias, Editors, Vol. 3, p. 55, VCH, Weinheim (1994).
- P. Allongue, V. Costa-Kieling, and H. Gerischer, *J. Electrochem. Soc.*, **140**, 1018 (1993).
- P. M. M. C. Bressers, S. A. S. P. Pagano, and J. J. Kelly, *J. Electroanal. Chem.*, **391**, 159 (1995).
- H. Morinaga, M. Suyama, and T. Ohmi, *J. Electrochem. Soc.*, **141**, 2834 (1994).
- J. S. Kim, H. Morita, J. D. Joo, and T. Ohmi, *J. Electrochem. Soc.*, **144**, 3275 (1997).